Analysis of the Partially-Filled d-Block Band of the Layered Metal LaI_2 and Probable Cause for the Absence of Structural Instability

Enric Canadell*

Laboratoire de Chimie Théorique (CNRS URA 506), Université de Paris-Sud, 91405 Orsay, France

Myung-Hwan Whangbo*

Department of Chemistry, North Carolina State University, Raleigh, North Carolina 27695-8204

Received July 8, 1993®

The electronic band structure of the layered metal LaI_2 was calculated by employing the extended Hückel tight binding method, and the orbital compositions of the partially filled bands were analyzed. The partially-filled bands are mainly composed of the La z^2 and $x^2 - y^2$ orbitals, but their relative contributions depend strongly on the wave vectors. Thus the Fermi surface is strongly warped so that LaI_2 does not possess an electronic instability typically expected for a system with a nested Fermi surface. The absence of a metal atom clustering in LaI_2 was discussed from the viewpoints of the strain and the preferential direction of metal–metal bonding of the square lattice. The Fermi surface has the shape of a warped-square cylinder running along the $\Gamma \rightarrow Z$ direction (i.e., perpendicular to the layer), and the cross-sectional area (taken perpendicular to $\Gamma \rightarrow Z$) oscillates between two slightly different values, so that the magnetoresistance of LaI_2 is predicted to exhibit angle-dependent oscillations.

Introduction

A low-dimensional metal often undergoes a metal-to-insulator or metal-to-metal phase transition that introduces an additional periodicity into the crystal lattice, which is commonly described as a charge density wave (CDW) instability.[1] Frequently, the latter is considered to occur when the Fermi surface of the metal is nested. The electronic instability arising from a nested Fermi surface gives rise to a periodic lattice distortion that opens a band gap at the Fermi level, and so it is analogous to a first-order Jahn–Teller instability in molecules. Recently, the concept of hidden nesting[2] was introduced to explain the occurrence of CDW instabilities in a number of low-dimensional metals, for which individual Fermi surfaces do not show any nesting.

The concept of Fermi surface nesting is extremely useful in dealing with the CDW phenomena of low-dimensional metals. However, it is crucial to recognize the fact that the presence of Fermi surface nesting is neither a sufficient nor a necessary condition for the observation of periodic lattice distortions in solids. For instance, $Na_3Cu_4S_4$ has very well nested Fermi surfaces[3a] but does not show any corresponding CDW instability down to ~ 10 K,[3b] probably because the phonon that couples with the electrons at the Fermi level induces a strong lattice strain.[3a] The Fermi surface of 2H-TaS_2 does have nesting,[2c] but the 3×3 distortion of 2H-TaS_2 is unrelated to this nesting and hence does not open a band gap at the Fermi level. This distortion is energetically favorable because it lowers the energy of the band levels (considerably below the Fermi level) where adjacent metal atoms have bonding interactions.[2c] Another example is the 2×2 distortion of 1T-$TiSe_2$, which arises from second-order Jahn–Teller distortions of the $TiSe_6$ octahedra constituting the $TiSe_2$ layers[2c] and is not driven by a Fermi surface nesting.

The layered halide LaI_2 is a metal.[4] Recently, Wilson and co-workers[5] carried out resistivity and magnetic susceptibility measurements for LaI_2, which show no trace of CDW phase transition down to ~ 10 K. They report that the Fermi surface of LaI_2, calculated by them on the basis of the LMTO–ASA method,[6] shows a very good nesting. The LaI_2 layer is made up of LaI_8 square prisms (**1**)by sharing their edges.[7] In the sense

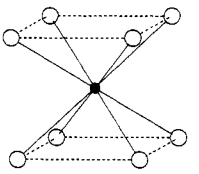

1

of prismatic coordination, the structure of the LaI_2 layer is similar to that of the 2H-TaS_2 layer made up of TaS_6 trigonal prisms. For the 2H-TaS_2 layer, the Fermi surface nesting does not lead to a corresponding CDW, so it may not be surprising that the LaI_2 layer does not show a CDW corresponding to the Fermi surface nesting. However, LaI_2 does not even show a metal atom clustering analogous to that found in 1T-TaS_2. To gain insight into these rather apparently puzzling observations, we study the electronic structure of LaI_2 on the basis of the extended Hückel

* Abstract published in *Advance ACS Abstracts,* December 15, 1993.

(1) For recent reviews, see: (a) *Electronic Properties of Inorganic Quasi-One-Dimensional Compounds*; Monceau, P., Ed.; Reidel: Dordrecht, The Netherlands, 1985; Parts I and II. (b) *Crystal Chemistry and Properties of Materials with Quasi-One-Dimensional Structures*; Rouxel, J., Ed.; Reidel: Dordrecht, The Netherlands, 1986. (c) *Structure Phase Transitions in Layered Transition Metal Compounds*; Motizuki, K., Ed.; Reidel: Dordrecht, The Netherlands, 1986. (d) *Low-Dimensional Electronic Properties of Molybdenum Bronzes and Oxides*; Schlenker, C., Ed.: Kluwer Academic Publishers: Dordrecht, The Netherlands, 1989. (e) Pouget, J. P. In *Semiconductors and Semimetals*; Conwell, E., Ed.; Academic Press: New York, 1988; Vol. 27, p 87.

(2) (a) Whangbo, M.-H.; Canadell, E.; Foury, P.; Pouget, J. P. *Science* **1991**, *252*, 96. (b) Canadell, E.; Whangbo, M.-H. *Chem. Rev.* **1991**, *91*, 965. (c) Whangbo, M.-H.; Canadell, E. *J. Am. Chem. Soc.* **1992**, *114*, 9587. (d) Whangbo, M.-H.; Ren, J.; Liang, W.; Canadell, E.; Pouget, J.-P.; Ravy, S.; Williams, J. M.; Beno, M. A. *Inorg. Chem.* **1992**, *31*, 4169.

(3) (a) Whangbo, M.-H.; Canadell, E. *Inorg. Chem.* **1990**, *29*, 1395. (b) Peplinski, Z.; Brown, D. B.; Watt, T.; Hatfield, W. E.; Day, P. *Inorg. Chem.* **1982**, *21*, 1752.

(4) Corbett, J. D.; Sallach, R. A.; Lokken, D. A. *Adv. Chem. Ser.* **1967**, *71*, 56.

(5) Burrow, J. H.; Maule, C. H.; Strange, P.; Tothill, J. N.; Wilson, J. A. *J. Phys. C: Solid State Phys.* **1987**, *20*, 4115.

(6) Skriver, H. L. *The LMTO Method*; Springer: Berlin, 1984.

(7) Warkentin, E.; Bärnighausen, H. Cited by: Hulliger, F. In *Structural Chemistry of Layer-Type Phases*; Lévy, F., Ed.; Reidel: Dordrecht, The Netherlands, 1976; p 247.

0020-1669/94/1333-0287$04.50/0

Table 1. Exponents ζ_i and Valence Shell Ionization Potentials H_{ii} for Slater Type Atomic Orbitals χ_i[a,b]

atom	χ_i	ζ_i	ζ_i'	H_{ii} (eV)
I	5s	2.679		−18.0
I	5p	2.322		−12.7
La	6s	2.14		−7.67
La	6p	2.08		−5.01
La	5d	3.78 (0.7763)	1.38 (0.4587)	−8.21

[a] H_{ii}'s are the diagonal matrix elements $\langle\chi_i|H^{eff}|\chi_i\rangle$, where H^{eff} is the effective Hamiltonian. In our calculations of the off-diagonal matrix elements $H_{ij} = \langle\chi_i|H^{eff}|\chi_j\rangle$, the weighted formula was used. For details, see ref 9b. [b] The 5d orbitals of La are given as a linear combination of two different Slater type orbitals, and each is followed by the weighting coefficient in parentheses.

tight binding (EHTB) method[8,9] and analyze the nature of its partially filled d-block bands in some detail. The atomic orbital parameters employed in our calculations are summarized in Table 1.

Crystal Structure and Local Bonding

For our analysis of the electronic band structure of LaI_2, it is necessary to briefly discuss the crystal structure of LaI_2[5,7] and the low-lying d-block levels of the La^{2+} (d^1) ions. By sharing their edges, LaI_8 square prisms **1** lead to an LaI_2 layer **2**. The top

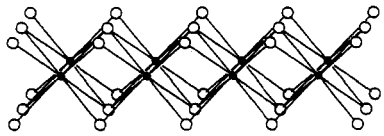

2

and side projection views of this layer can be represented by **3a** and **3b**,respectively. In a unit cell, the LaI_2 lattice has two identical

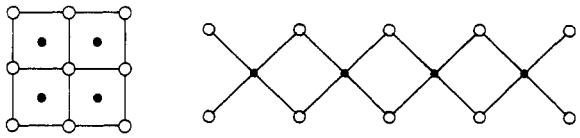

3a **3b**

LaI_2 layers arranged in such a way that, in a top projection view, the La atoms of one layer sit on top of the I atoms of the adjacent layers. Thus, a side projection view of the LaI_2 lattice can be presented by **4**. It is important to point out that, except for the

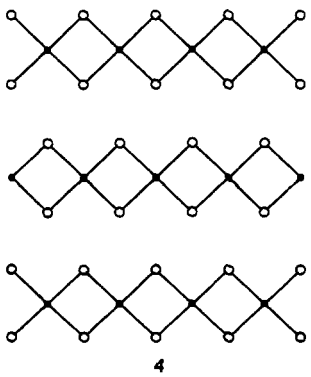

4

unpublished work by Warkentin and Bärnighausen cited in Hulliger's review,[7] all the structural details of LaI_2 have never been published. Therefore, there is some concern as to the correctness of the LaI_2 structure. As in the study of Wilson et al.,[5] our work will be based on the LaI_2 structure of Warkentin and Bärnighausen.

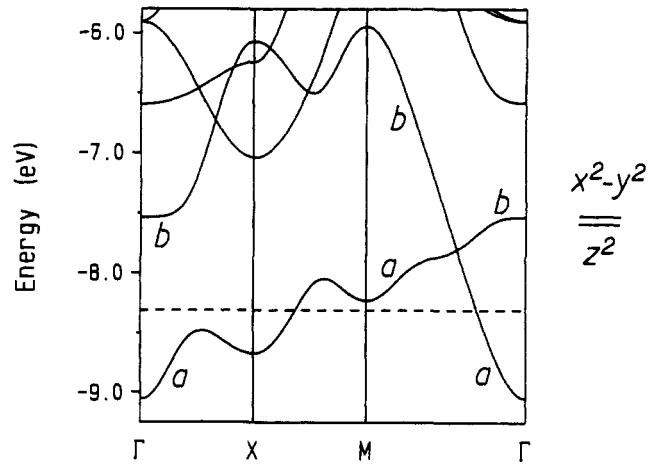

Figure 1. Dispersion relations of the bottom portion of the d-block bands calculated for a single LaI_2 layer. The dashed line refers to the Fermi level. Γ = (0, 0), X = ($a^*/2$, 0), Y = (0, $b^*/2$), and M = ($a^*/2$, $b^*/2$). The two energy levels on the right-hand side refer to the z^2 and $x^2 - y^2$ levels calculated for an isolated LaI_8^{6-} cluster.

As shown in **5a** and **5b**, the d-orbital splitting pattern of a square prism (ML_8) coordination is opposite to that of a trigonalprism (ML_6) coordination. The bottom two d-block levels

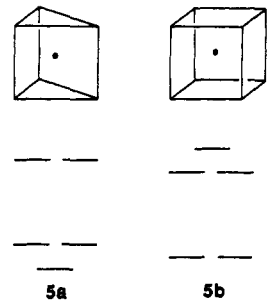

5a **5b**

of an ML_8 square prism are dominated by the metal z^2 (**6a**) and $x^2 - y^2$ (**6b**)orbitals, where the antibonding contributions of the

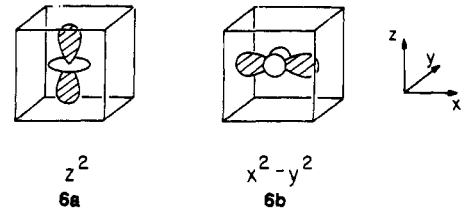

6a **6b**

surrounding ligand orbitals are not shown for simplicity. Because the d-electron count is very low in LaI_2 (i.e., d^1), only the d-block bands derived from these two orbitals become partially filled, thereby governing the transport properties of LaI_2.

Nature of the Partially Filled d-Block Bands of a Single LaI_2 Layer

The dispersion relations of the bottom portion of the d-block bands calculated for a single LaI_2 layer are shown in Figure 1, where the dashed line is the Fermi level and the two energy levels on the right-hand side refer to the z^2 and $x^2 - y^2$ levels of an isolated square prism LaI_8^{6-} unit. The dispersion relations of bands a and b, in the vicinity of the z^2 and $x^2 - y^2$ levels of LaI_8^{6-}, are quite complex. This signifies the occurrence of strong wave-vector-dependent hybridization between the z^2 and $x^2 - y^2$ orbitals. To examine the nature of this hybridization and its consequence, we carry out electronic band structure calculations for a single

(8) Whangbo, M.-H.; Hoffmann, R. *J. Am. Chem. Soc.* **1978**, *100*, 6093.
(9) (a) Hoffmann, R. *J. Chem. Phys.* **1963**, *39*, 1397. (b) Ammeter, J. H.; Bürgi, H.-B.; Thibeault, J.; Hoffmann, R. *J. Am. Chem. Soc.* **1978**, *100*, 3686.

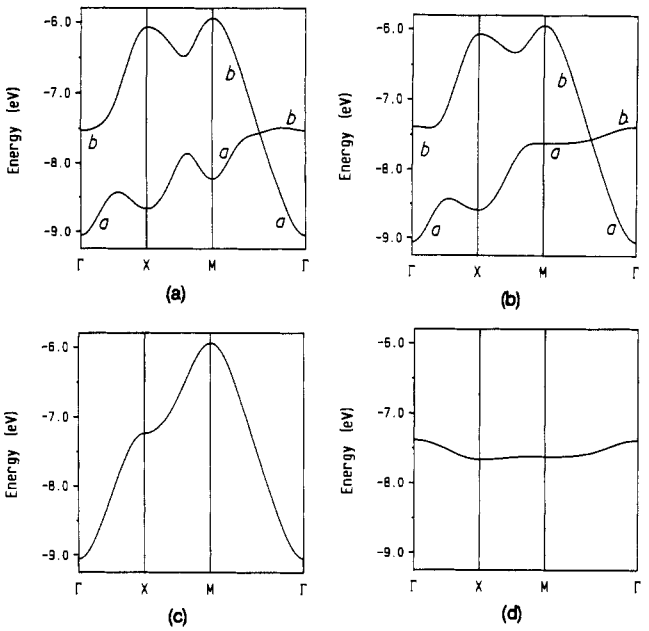

Figure 2. Dispersion relations of the bands calculated for a single LaI_2 layer by employing all the orbitals of I but a limited number of orbitals for La: (a) only the $x^2 - y^2$, z^2, and s orbitals; (b) only the $x^2 - y^2$ and z^2 orbitals; (c) only the $x^2 - y^2$ orbital; (d) only the z^2 o rbital.

LaI_2 layer by employing all the orbitals of I but a limited number of orbitals for La as specified below: (a) only the $x^2 - y^2$, z^2, and s orbitals, (b) only the $x^2 - y^2$ and z^2 orbitals, (c) only the $x^2 - y^2$ orbital, and (d) only the z^2 orbital. Figure 2 summarizes the dispersion relations of the bands (only within the energy window of Figure 1) calculated for cases a–d.

From Figures 1 and 2a it is evident that bands a and b arise essentially from the $x^2 - y^2$, z^2, and s orbitals of La and the I orbitals. Parts a and b of Figure 2 show that the primary role of the La s orbital is to slightly stabilize band a only in the vicinity of M, but the extent of the stabilization is not large enough to push band a below the Fermi level. Namely, the essential features of bands a and b of Figure 1 are derived from the $x^2 - y^2$ and z^2 orbitals of La and the I orbitals, and they are not affected by the La s orbital. Figure 2c shows a wide two-dimensional (2D) band resulting from the $x^2 - y^2$ orbitals alone. The very narrow band resulting from the z^2 orbital alone (Figure 2d) occurs in the middle of the wide 2D band of Figure 2c. From the comparison of parts b–d of Figure 2, it is clear that hybridization of the $x^2 - y^2$ and z^2 orbitals is responsible for the formation of bands a and b of a LaI_2 layer.

Nature of Band Orbital Hybridization

We now examine the orbital components of bands a and b of LaI_2 at the wave vector points Γ, X, Y, and M. At Γ, the Bloch orbitals derived from the $x^2 - y^2$ and z^2 orbitals are given by **7a** and **7b**, respectively. In **7a**, the $x^2 - y^2$ orbitals have metal–metal

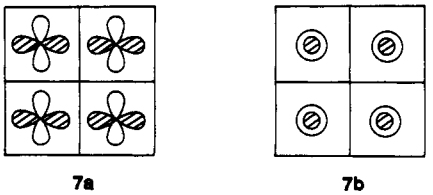

7a **7b**

bonding interactions in two directions. In addition, the nodal planes of **7a** contain the ligands so that the ligand orbitals do not mix into, and hence do not raise, level **7a**. The z^2 orbitals repeat in-phase in **7b**, but direct metal–metal bonding is not effective. In **7b**, the ligand orbitals mix into, and hence raise, level **7b** to the position of the z^2 level of an isolated LaI_8^{6-} (see the right-hand side of Figure 1). At Γ, **7a** and **7b** are different in symmetry, so that they do not mix. Thus, **7a** and **7b** represent bands a and b of Figure 2b at Γ, respectively.

At M, the Bloch orbitals derived from the $x^2 - y^2$ and z^2 orbitals are given by **8a** and **8b**, respectively. The $x^2 - y^2$ orbitals have

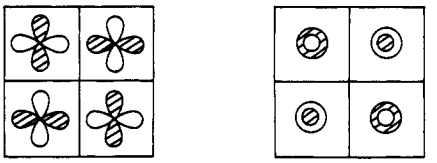

8a **8b**

metal–metal antibonding interactions in **8a** in two directions, while the antibonding interactions between the z^2 orbitals in **8b** are not effective. Hence, **8b** is lower in energy than **8a**. At M, **8a** and **8b** do not mix due to their different symmetries, so that **8a** and **8b** represent bands b and a of Figure 2b at M, respectively.

At X, the Bloch orbitals derived from the $x^2 - y^2$ and z^2 orbitals are given by **9a** and **9b**, respectively. In **9a**, the $x^2 - y^2$ orbitals

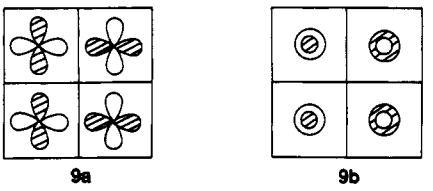

9a **9b**

have metal–metal antibonding interactions along the *a*-direction but bonding interactions along the *b*-direction, so that **9** is a "nonbonding" level, as is **9b**. Since the symmetries of **9a** and **9b** are the same, they interact so that their plus and minus combinations (**10a** and **10b**,respectively) are the proper band

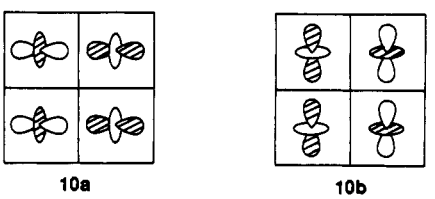

10a **10b**

orbitals. This orbital mixing hybridizes the metal orbitals in such a way that strong metal–metal bonding occurs along the *b*-direction in **10b**, while strong metal–metal antibonding occurs along the *a*-direction in **10a**. Hence, **10b** and **10a** represent bands a and b of Figure 2b, respectively. Likewise, at Y, bands a and b of Figure 2b are represented by **11b** and **11a**, respectively. (It is interesting to note that the 2H-TaS_2 system with trigonal prismatic coordination also exhibits metal–metal σ bonding by hybridization.[2c])

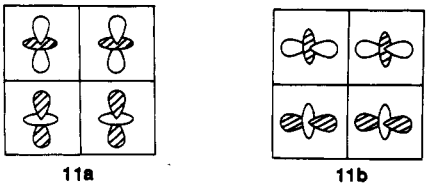

11a **11b**

The above orbital analysis reveals that the nature of bands a and b of Figure 2b depends strongly on the wave vector. Band a is given by the $x^2 - y^2$ orbitals at Γ, by z^2 orbitals at M, and by the hybrid orbitals of $x^2 - y^2$ and z^2 at X and Y. This finding originates from the topological aspects of the square lattice of metal atoms in square prismatic coordination. This wave-vector-

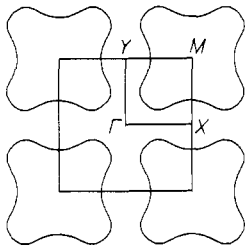

Figure 3. Fermi surface calculated for a single LaI_2 layer. $\Gamma = (0, 0)$, $X = (a^*/2, 0)$, $Y = (0, b^*/2)$, and $M = (a^*/2, b^*/2)$. The pockets at M and its equivalent points are empty.

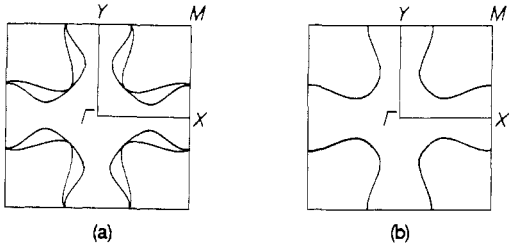

Figure 4. Cross sections, perpendicular to the $\Gamma \rightarrow Z$ direction, of the Fermi surface calculated for the 3D LaI_2 lattice at the c^*-heights of (a) 0 and (b) $c^*/2$ respectively.

dependent hybridization phenomenon is also found in a hexagonal lattice of metal atoms in trigonal prismatic coordination (e.g., 2H-TaS_2).[2c]

Fermi Surface

Figure 3 shows the Fermi surface calculated for band a of a LaI_2 layer. This Fermi surface is the same as that reported by Wilson and co-workers[5] only in that empty pockets are present at M and its equivalent points. In our results, the empty pockets have a shape significantly warped from a square, so that there is no Fermi surface nesting. For a square lattice 2D metal, the Fermi surface of an isotropic band (i.e., that arising from the s, z^2, $x^2 - y^2$, or xy orbital) is nested when the band is half-filled. As described in the previous section, band a of a LaI_2 layer has orbital compositions which depend strongly on wave vector (e.g., $x^2 - y^2$ at Γ, z^2 at M, and the hybrid of $x^2 - y^2$ and z^2 at X and Y). Because of this complex orbital mixing, the correct Fermi surface of this band is more likely to be strongly warped, as found in our study, than square-like, as obtained by Wilson and co-workers.[5]

As noted earlier, the three-dimensional (3D) LaI_2 lattice has two LaI_2 layers per unit cell. The band dispersion relations calculated for the 3D lattice (with the tetragonal unit cell) are quite similar to those of a single LaI_2 layer, except for the doubling of the bands due to a doubled unit cell size, and hence they are not shown. Two cross sections of the Fermi surface calculated for the 3D LaI_2 lattice are shown in Figure 4. Because of the unit cell doubling, two Fermi surfaces are present. At the c^*-height of 0, the two Fermi surfaces are split sightly because of the weak interlayer interactions (Figure 4a). At the c^*-height of $c^*/2$, the two Fermi surfaces become identical due to symmetry (Figure 4b). Therefore, in an extended-zone representation, the 3D Fermi surface has the shape of a warped-square cylinder running along the $\Gamma \rightarrow Z$ direction (i.e., perpendicular to the LaI_2 layer). The cross-sectional area of this cylinder (taken perpendicular to $\Gamma \rightarrow Z$) oscillates between two slightly different values as the wave vector varies along the $\Gamma \rightarrow Z$ direction. Consequently, it is predicted that the magnetoresistance of LaI_2 should exhibit angle-dependent oscillations.[10]

Absence of Metal Atom Clustering

The Fermi surface of the 2H-TaS_2 system is nested, but its 3 × 3 modulation is unrelated to the nesting.[2c] The electronic

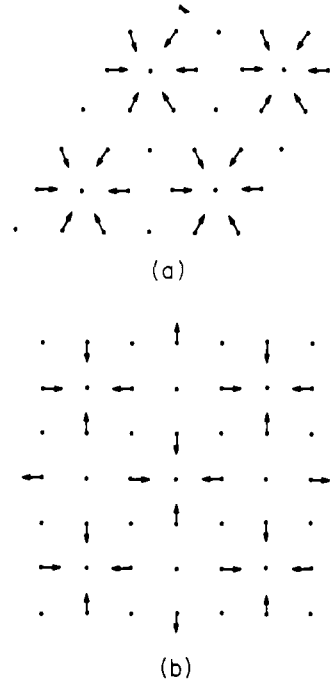

Figure 5. (a) 3 × 3 clustering of metal atoms in 2H-TaS_2 proposed by Brouwer and Jellinek.[11] (b) Hypothetical 4 × 4 clustering of metal atoms in LaI_2.

structures of 2H-TaS_2 calculated for the lattice with and without the 3 × 3 modulation show that the 3 × 3 modulation is energetically favorable because the metal–metal-bonding levels, which occur below the Fermi level, are further stabilized by the metal atom clustering (Figure 5a[11]) associated with the modulation.[2c] Since both 2H-TaS_2 and LaI_2 layers have metal ions in prismatic coordination, it is worthwhile to consider why a metal atom clustering similar to that of 2H-TaS_2 is not feasible. A metal atom clustering is inevitably accompanied by lattice strain so that, to compensate for this strain, it is necessary to gain a large amount of stabilization in electronic energy. Therefore, it would be energetically more favorable if more metal atoms participate in a clustering process. In the hexagonal lattice (Figure 5a), there are nine metal ions per unit cell, and seven of them participate in the clustering.

Figure 5b shows a hypothetical metal atom clustering in a square lattice. The metal atoms are shown to move only along the shorter metal–metal-contact direction because, as discussed in the previous section, metal–metal σ bonding can be achieved only along these directions (see **10b** and **11b**). With this constraint, any pattern other than the one in Figure 5b is found to involve less metal atoms in clustering. In Figure 5b, there are 16 metal atoms per unit cell, and only 10 of them are involved in the clustering. Thus, in percentage, less metal atoms are involved in clustering in the square than in the hexagonal lattice. Therefore, on the basis of the electronic energy gain, the metal clustering is expected to be less favorable in the LaI_2 lattice than in the 2H-TaS_2 lattice, in agreement with the finding that a metal atom clustering occurs in 2H-TaS_2 but not in LaI_2.

It should be noted that 2H-MX_2 (d^1) systems 2H-TaS_2, 2H-$TaSe_2$, and 2H-$NbSe_2$ all show a 3 × 3 modulation, but 2H-NbS_2 does not.[12] The phase transition temperature for the 3 × 3 modulation of 2H-MX_2 increases with increasing M–X bond length.[12] Furthermore, the extent of distortion in a d^2 1T-MX_2 layer system (i.e., the one made up of MX_6 octahedra) is found to increase with increasing M–X bond length.[13] These obser-

(10) Yamaji, K. *J. Phys. Soc. Jpn.* **1989**, *70*, 1189.
(11) Brouwer, R.; Jellinek, F. *Physica B* **1980**, *99*, 51.
(12) For a review, see: DiSalvo, F. J. In *Electron-Phonon Interactions and Phase Transitions*; Riste, T., Ed.; Plenum: New York, 1977; p 107.
(13) Rovira, C.; Whangbo, M.-H. *Inorg. Chem.* **1993**, *32*, 4094.

vations imply that an MX_2 layer with a long, polarizable M–X bond can lower its electronic energy by distortion without causing a great lattice strain. Then, the absence of a 3×3 modulation in 2H-NbS_2 can be attributed to the short Nb–S bond and the associated hardness of the lattice. Layered halide d^1 metals CeI_2, PrI_2, and NdI_2 are isostructural with LaI_2.[4,7] Of these halides, LaI_2 should have the longest metal–ligand bond length. Therefore, in terms of lattice strain, a metal atom clustering would be less favorable for CeI_2, PrI_2, and NdI_2 than for LaI_2. Since a metal clustering is absent in LaI_2, it is unlikely that a metal clustering will occur in CeI_2, PrI_2, and NdI_2.

Concluding Remarks

Our electronic band structure calculations for LaI_2 show that the major components of its partially-filled band are the La z^2 and $x^2 - y^2$ orbitals, and their relative contributions depend on wave vectors. As a consequence, the Fermi surface is strongly warped, and no nesting is present. Thus, LaI_2 should not possess an electronic instability typically expected for a system with a nested Fermi surface, in agreement with experiment. The absence of a metal atom clustering in LaI_2 appears to originate from the facts that the metal–metal bonding can occur only along the shorter metal–metal directions and that the square lattice does not allow many metal atoms to participate in clustering. Consideration of the lattice strain associated with the metal–ligand bond length suggests that a metal atom clustering will be also absent in the isostructural d^1 metals CeI_2, PrI_2, and NdI_2. The Fermi surface of the 3D LaI_2 lattice has the shape of a warped-square cylinder running along the $\Gamma \rightarrow Z$ direction, and the cross-sectional area (taken perpendicular to $\Gamma \rightarrow Z$) oscillates between two slightly different values. Consequently, the magnetoresistance of LaI_2, and also its isostructural series CeI_2, PrI_2, and NdI_2, is expected to exhibit angle-dependent oscillations. For the characterization of the physical properties of LaI_2, it is imperative to synthesize pure samples of LaI_2 and accurately determine its crystal structure.

Acknowledgment. This work was supported by the U.S. Department of Energy, Office of Basic Sciences, Division of Materials Sciences, under Grant DE-FG05-86ER45259, by NATO, Scientific Affairs Division, under Grant CRG 910129, and by the Centre National de la Recherche Scientifique, France. We thank one of the reviewers of this work for his invaluable comments.